A Molecular Counterpart to the Herbig-Haro 1-2 Flow

Amaya Moro-Martín & José Cernicharo

Instituto de Estructura de la Materia, Dpto. de Fisica Molecular, CSIC, Serrano 121, E-28006 Madrid, Spain

email:amaya, cerni@astro.iem.csic.es

and

Alberto Noriega-Crespo

Infrared Processing and Analysis Center, CalTech-JPL, Pasadena, CA 91125, USA

email: alberto@ipac.caltech.edu

and

Jesús Martín-Pintado

Observatorio Astronómico Nacional. Apartado 1143, E-28800 Alcalá de Henares. Spain

email: martin@oan.es

Received ______________________; accepted ______________________

ABSTRACT

We present high angular resolution (12″-24″) and high sensitivity ^{12}CO and ^{13}CO J = 2-1 and J = 1-0 observations of the HH 1-2 outflow. The observations show the molecular counterpart, moving with a velocity of $\simeq$ 30 km s^{-1}, of the optical bipolar system driven by the VLA 1 embedded source. Along the optical jet there are certain regions where the molecular gas reaches deprojected velocities of 100 - 200 km s^{-1}, and that we interpret as the molecular jet. The bipolar CO outflow has a length of $\sim$ 260″ with a curved morphology towards the North where it extends beyond the HH 1 object ($\simeq$ 120 ″) .

Two new molecular outflows have been detected, one arising from IRAS 05339-0647 which excites the HH 147 optical flow and another powered by VLA 2 which drives the HH 144 optical outflow. The molecular outflow driven by the VLA 3 source is also clearly detected and spatially resolved from the VLA 1 main outflow.

Subject headings: ISM: individual (HH 1-2)— ISM: jets and outflows— ISM: molecules— stars: formation

1. Introduction

A causality connection between molecular outflows and the optical proto-stellar jets is becoming stronger as the number of objects with a consistent set of radio, IR and optical observations has grown. High velocity CO emission is seen to be correlated, kinematically and morphologically, for example, with the optical emission in the HH 111 outflow (Cernicharo & Reipurth 1996, hereafter CR96). In HH 111, high velocity CO bullets are detected far away from the optical jet and along the same flow line, which indicates that the optical jet and molecular outflow coexist spatially and probably also in time (CR96). Both are manifestations of the physical processes occurring in the neighborhood of a nascent star which contribute to dissipate part of its surrounding dense material.

The HH 1-2 system is one of the brightest Herbig-Haro flows, but despite various attempts an associated, collimated molecular outflow has not been clearly identified (Martín-Pintado & Cernicharo 1987, hereafter MPC87; Torrelles et al. 1994; Chernin & Masson 1995, hereafter CM95; Choi & Zhou 1997; Correia et al. 1997; and see $3). It has been suggested (CM95) that the difficulty in detecting and resolving the CO outflow is due to the fact that the CO emission is weak and oriented almost in the plane of the sky ($\sim 10°$, Noriega-Crespo et al. 1989), and confusion with the background emission is very important. The source driving the HH 1-2 flow is the embedded object VLA 1 (Pravdo et al. 1985; Rodriguez et al. 1990), which powers a highly collimated atomic/ionic jet that interacts with the surrounding medium exciting the HH 1 and 2 objects. The flow velocities of the atomic/ionic jet and HH 1-2 are $\sim 200 - 380$ km s^{-1} (Herbig & Jones 1981; Raga et al. 1990; Reipurth et al. 1993; Eislöffel et al. 1994). The similar morphology of the optical and the vibrationally excited H_2 2.12 μm emission (Davis et al. 1994; Noriega-Crespo & Garnavich 1994) indicates a relationship between the atomic/ionic and the molecular gas dynamics, a conclusion further supported by the measured proper motions (Noriega-Crespo et al. 1997). It has been suggested (MPC87) that the distribution of high density gas around HH 1-2 is placed along the walls of the cavity produced by the optical jet through its interaction with the ambient quiescent gas. In this Letter we present high resolution and sensitivity maps of the ^{12}CO and ^{13}CO emission which clearly show, despite the multiple outflows around the HH 1-2 system, the fast and collimated CO emission along the stellar jet flow axis.

2. Observations

The observations were performed with the 30m IRAM radio telescope at different runs during the 1987-1999 period, with a 12″ spatial resolution. The final wide coverage maps were obtained in May 1998 and selected positions along the optical jet in January 1999. Three SIS receivers at 3, 2 and 1mm were used simultaneously with receiver temperatures at 100, 100 and 150 K, respectively. The 3mm and 1mm receivers were tuned to the frequencies of CO, ^{13}CO J=1-0 and J=2-1 lines respectively, while the 2mm receiver was used to observe the J=3-2 line of CS (these data will presented elsewhere). The spectrometers were two 512 $\times$ 1 MHz filter banks, one 256$\times$100 KHz filter bank, and an autocorrelator with 2048 channels and spectral resolution of 37 KHz. Calibration was performed by using two absorbers at different temperatures and by deriving the atmospheric attenuation from the atmospheric emissivity. In all runs several common positions were observed to ensure calibration consistency for all data. Intensity differences never exceeded 10%. A region of 316″ $\times$ 440″, centered on the VLA 1 source, was covered. The maps are obtained by fast rastering observations with a spacing of 7″, followed by a pointing and focus check. Figure 1 shows some representative CO and ^{13}CO spectra at selected positions along the optical jet of the HH 1-2 system (position (0″,0″) corresponds to the VLA 1 source). The maximum emission of the background cloud is at a velocity of $\simeq$ 9.5 km s^{-1} in agreement with previous studies (see, e.g., MPC87; Correia et al. 1997). Figures 2a and 2b show the integrated intensity of the ^{12}CO and ^{13}CO J=2-1 lines for different velocity ranges. Finally, Figure 2c shows the superposition of the ^{12}CO J=2-1 emission, between 11 and 11.5 km s^{-1} (contours) and the [SII] 6717/31 optical image, covering a field of $2'$.

3. Results and Discussion

Previous observations of HH 1-2 in ^{12}CO were unable to distinguish the morphology of the outflow arising from the VLA 1 source due to their limited spatial resolution (CM95). Two recent studies nevertheless show evidence of a CO outflow along the symmetry axis of the optical jet. In the ^{12}CO $J = 3 - 2$ study of Correia et al. (1997), the integrated intensity shows redshifted (V$= 14 - 20$ km s^{-1}) and blueshifted (V $= 0 - 5$ km s^{-1}) emission centered on VLA 1 just as one would expect for an outflow very close to the plane of the sky. A similar conclusion was reached by Choi & Zhou (1997) from the integrated spectrum within $20''$ around VLA 1 of the same transition. They detected a blue wing reaching up to V $= -6$ km s^{-1} and red wing up to V $= 28$ km s^{-1}. The data presented here covers a larger field of view, with better angular resolution and sensitivity, which permit us to distinguish the presence of a low radial velocity narrowly collimated outflow along the symmetry axis of the atomic jet and the presence of high velocity gas at some positions along the jet. There is a wealth of detail in the ^{12}CO and ^{13}CO maps, so we will focus only on the most relevant aspects in these data in subsections 3.1 to 3.3. The distribution of other molecular outflows in the region is briefly discussed in subsection 3.4.

3.1. The low velocity gas

Figure 2a displays the ^{12}CO emission at different velocity ranges in a gray scale where darker areas mean a higher intensity. These maps show that the emission between 8 and 14 km s^{-1}around the VLA 1 source is narrow. Figure 2c corresponds to the integrated emission over a velocity range of 11 - 11.5 km s^{-1}, avoiding most of the background cloud emission, that stresses the highly collimated CO morphology along the optical jet flow, bounded by the optical HH 1-2 objects. The elongated structure seen from 4 to 8 km s^{-1} north of HH 1, at around (-40″, 100″), would be the blue-shifted counterpart of the molecular jet connecting VLA 1 and HH2. A red-shifted ^{12}CO intensity enhancement from 10.5 to 14 km s^{-1} (see Figure 2a) at around (-10″, 15″) coincides with the position and the extension of the optical jet. Indeed the strongest emission corresponds to the position of a smaller working surface observed in the H_2 2.12 μm emission (Noriega-Crespo et al. 1997). If the CO emission is produced by the interaction of a working surface with dense material, then the redshifted emission could be a consequence of the wide velocity dispersion expected in such structures (Böhm & Solf 1992). In addition, the ambient medium around the jet could have a very axisymmetric distribution. The gas in front of the jet could contribute with a small column density (the jet is visible), while the gas behind the optical jet (redshifted gas) could have larger column densities and densities. A slightly expanding cone around the jet will be seen mainly at redshifted velocities.

The mass of the HH 1-2 low velocity molecular outflow can be estimated ¿from the CO J=1-0 and J=2-1 line intensities. The J=2-1/J=1-0 intensity ratio (deconvolved for the different beam sizes) shows a clear increase from 1 in the ambient cloud to 1.4-1.7 along the optical jet (i.e. not very different from that observed in HH 111 (CR96)). If we assume a thermalised optically thin emission this ratio corresponds to a kinetic temperature of 30 K. However, due to the low velocity difference between the CO ambient gas and the molecular outflow, it is difficult to separate their contributions and to estimate the mass of the molecular outflow. From a map of the total integrated intensity, which shows a clear enhancement of the CO emission in the direction of the optical system (see individual panels in Figure 2a and Figure 2c), we can estimate the CO integrated intensity associated with the jet by removing the background emission. We obtain an average value for W(CO(2-1)) of $\simeq$5 K km s^{-1}. For a distance of 440 pc and by using the W(CO)/Av ratio found by Cernicharo & Guélin (1987) we derive a mass of 0.1 $M_\odot$ for each lobe of the molecular outflow. Since this mass is larger than that associated with just high velocity gas, as e.g. in HH 111 (CR96), we suspect that a low velocity component is included in our estimates, due perhaps to the walls of an expanding cavity around the optical jet (CR96;Cernicharo et al. 1997).

The high velocity collimated CO emission associated with the outflow is observed at a low intensity level and over a narrow velocity range. It begins to show up at 10.5-11 km s^{-1}, but it is only at 11-11.5 km s^{-1} that it is clearly detected. This gas has not been observed in previous studies due to their limited spatial resolution and sensitivity. In HH 111 the cavity walls are detected over a velocity range of $\simeq$ 10-15 km s^{-1} (CR96). In HH 1-2 the range is only $\simeq$ 4-5 km/s, but if the projection angle is closer to its estimated lower limit ($\sim 5°$) then both jets have similar velocity ranges. We have made some crude estimates for the volume density and CO column density from a LVG code, for the velocity range 11-12.5 km s^{-1} alone and assuming T_K = 30 K, we obtain a mass of 0.025 $M_\odot$ in each lobe in HH 1 -2. Taking into account that the total velocity coverage of the molecular outflow is $\simeq$6-8 km s^{-1} the above mass estimates are in good agreement

3.2. The high velocity gas

Although the HH 1-2 system is nearly in the plane of the sky we have found indications of high velocity gas at several positions along the optical jet. The top panel of Figure 1 at (48″,-60″), right on the HH 2 object, displays a large velocity dispersion, as a result of the strong shock experienced by the jet in this region. At (12″,-24″) a bright and extended ^{12}CO red wing is clearly detected, reaching up to deprojected velocities of $\sim$ 100 - 200 km s^{-1}(for a 5 - 10° angle). This wing remains in the two following panels, at (-12″,12″) and (0″,0″), and belongs to the high velocity CO gas in the jet. The jet blue wing is faint but is detected at

(-12″, 12″) and (-12″, 24″), reaching a deprojected velocity of $\sim 60 - 120$ kms $^{-1}$. The high velocity wings disappear in the last panel at (-36″, 60″) ahead of HH 1.

The high sensitivity data shown in Figure 1 correspond to selected positions and do not cover the full spatial extent of the jet. Hence, we can not determine if we are observing continuous high velocity gas along the jet or discreet bullets as in HH 111 (CR96). ¿From the observed ^{12}CO J=2-1 and J=1-0 intensities we can estimate the mass of the high velocity gas at each position by assuming a kinetic temperature for that gas of 60 K, similar to that in other outflows. We derive masses between 1-5 10^{-4} $M_{\odot}$ which are typical of bullets and extremely high velocity gas in young low-mass star forming regions (Bachiller et al., 1991; Bachiller & Cernicharo 1990; Bachiller 1996). As in the case of HH 111, the momentum and the mass associated with the high velocity gas seems to be enough to drive the low velocity gas in the cavity walls. We have searched for bullets, similar to those found in the HH 111 jet, further away of the HH objects without success. The more dense ambient medium in HH 1-2 when compared to HH 111, where the jet and the bullets are emerging into a very low density gas and escaping from the cloud, makes the identification of well spatially resolved discrete emission very difficult.

3.3. The effect of the jet on the molecular cloud

At velocities between 2 to 8 km s^{-1} and at $\simeq 10$ ″ SE from HH 2 there is a bright ^{12}CO emission which could be due to high density molecular gas struck by the jet. A similar intensity enhancement is also detected in the ^{13}CO observations (Figure 2b). The absence of the ambient emission in ^{13}CO at 9.5 km s^{-1} and at higher velocities could be interpreted precisely as the removal of the molecular gas from this region by the jet. The overall morphology seen in the ^{13}CO J=2-1 line is very different ¿from the corresponding line of the main isotope. The molecular outflow seen in CO (see Figures 1 and 2a) is not detected in the ^{13}CO line.

We detect a blue-shifted 'clump' ahead of HH 2 (see panel 1 of Figure 2b) that seems to be accelerated. This suggests that the observed optical bow shocks are not the terminal working surfaces of the outflow (Ogura 1995), but tracers of a more recent outburst event. If so, the clump is not the 'cloudlet' detected in HCO^+(Davis et al. 1990), but rather gas accelerated by the jet flow.

Another remarkable feature is the arc shape structure observed in ^{13}CO at 10-12 km s^{-1} arising near VLA 1 (Figure 2b) and that extends $\sim 180''$ SW. This emission has been seen in other molecules (see Cernicharo 1991) and it could be tracing low velocity gas from a cavity seen edge-on. The arc disappears at higher velocities (except around VLA 1), and its overall velocity field does not seem to be that of a rotating toroid, as suggested by Marcaide et al. (1988) and Torrelles et al. (1994). There is an off-center filamentary structure nearly parallel to the atomic jet axis and slightly red-shifted (see panel 3 of Figure 2b), which extends beyond the optical knots of HH 1, tracing perhaps the interaction of the outflow with the environment (i.e, the cavities discussed by MPC87).

3.4. Other Outflows around VLA 1

In addition to the molecular gas associated with HH 1-2 discussed above, our data also indicate the presence of several molecular outflows in the region. Previous studies (CM95) were not able to separate the outflow from VLA 1 from the brighter and more massive VLA 3 outflow. The higher resolution of our data makes this distinction possible, as it is clearly shown in Figure 2a. The blue lobe, between 2 and 4 km s^{-1}, is found north of VLA 3, while the red lobe, from 12 to 16 km s^{-1}, is south. The VLA 3 source is located at (-60$''$, 45$''$) with respect to VLA 1. The velocities are consistent with the ones derived by CM95, 0-4.5 and 12-18 km s^{-1} for the blue and red lobe respectively. The ^{12}CO J=2-1 observations between 10 and 16 km s^{-1} show an extended conical structure, with the apex close to the position of the near infrared IRAS 05339-0647 source $\sim 1'$ NE of HH 1 and at $2'$ south of V380 Ori. Two HH objects are also found near this source, HH 147 A-B. The proper motions derived by Eislöffel et al. (1994) show that the HH 147 outflow points towards the SW at a position angle of 230°, and away from IRAS 05339-0647. The maps in Figure 2a with velocities between 4 and 8 km s^{-1} present some ^{12}CO J=2-1 emission engulfing the region around the optical HH 147 A-B objects in an elongated structure oriented SW and could correspond to the molecular counterpart. In Figure 2c there is also some ^{12}CO emission along the HH 144 optical flow (Reipurth et al. 1993) and it probably represents the molecular counterpart to this outflow arising from VLA 2 and oriented E-W. This ^{12}CO emission outside the HH1-2 main axis is seen at velocities ranging from 10.5 to 12 km s^{-1} in Figure 2a.

4. Conclusions

In the HH 1-2 outflow the bulk of the ^{12}CO gas ($\sim 0.1 M_{\odot}$) is moving at deprojected velocities of 20-30 km s^{-1}. It is very likely that some of the ^{12}CO emission arises from the cavity walls excavated by the jet, but there must be a contribution from the molecular jet itself. The presence of clear traces ($\sim 10^{-4} M_{\odot}$) of high velocity molecular gas moving at 100-200 km s^{-1} reinforces this idea. There are few examples of bipolar outflows where it has been possible to observe simultaneously the high velocity molecular gas associated with the highly supersonic atomic/ionic gas. The HH 111 outflow (CR96) and now the HH 1-2 outflow are systems where the optical jet, the warm collimated H_2 gas and the high velocity ^{12}CO gas are coexisting. The fact that most of the known optical jets are in the plane of the sky makes it difficult to detect their associated molecular jets. The present results and those obtained by CR96 suggest that high velocity molecular gas may be present in other optical outflows, perhaps even in the form of "bullets". In addition, associated to this gas there is a low velocity molecular component along the cavity walls excavated by the supersonic atomic/ionic jet.

acknowledgements : We thank the referee, Bo Reipurth, for his critical and careful reading of the manuscript. We thank Spanish DGES for support under grants PB96-0883, PNIE98-1351, and PB96-104.

REFERENCES

Bachiller, R., & Cernicharo 1990, A&A, 239, 276

Bachiller, R., Martin-Pintado, J., & Fuente, A. 1991, A&A, 243, 21

Bachiller, R., 1996, ARAA, 34, 111

Böhm, K.H., & Solf, J. 1992, AJ, 104, 1193

Cernicharo, J. & Guélin, M. 1987, A&A, 176, 299

Cernicharo, J. 1991 in "The Physics of Star Formation and Early Stellar Evolution", eds C.J. Lada & Kylafis, D., p287

Cernicharo, J., & Reipurth, B. 1996, ApJ, 460, L57

Cernicharo, J., Neri, R. & Reipurth, B. 1997, in "Herbig-Haro Outflows and the Birth of Low Mass Stars", page 141; ed Bo Reipurth and C. Bertout. Kluwer Academic Press.

Chernin, L. M. & Masson, C.R. 1995, ApJ, 443, 181

Choi, M. & Zhou, Sh. 1997, ApJ, 477, 754

Correia, J.C., Griffin, M., & Saraceno, P. 1997, A&A, 322, L25

Davis, C. J., Dent, W. R. F., & Bell Burnell, S. J. 1990, MNRAS, 244, 173

Davis, C. J., Eislöffel, J., & Ray, T. P. 1994, ApJ, 426, L93

Eislöffel, J., Mundt, R., & Böhm 1994, AJ, 108, 104

Herbig, G. H., & Jones, B. F. 1981, AJ, 86, 1232

Martín-Pintado J., Cernicharo J. 1987, A&A, 176, 27

Marcaide, J.M., Torrelles, J.M., Güsten, R., Menten, K. M., Ho, T.P.T., Moran, J.M., & Rodrıguez, L.F., 1988, A&A, 197, 235

Noriega-Crespo, A., Böhm, K.-H. & Raga, A.C. 1989 AJ, 98, 1388

Noriega-Crespo, A., Calvet, N., & Böhm, K.-H. 1991 ApJ, 379, 676

Noriega-Crespo, A., & Garnavich, P. M. 1994, AJ, 108, 1432

Noriega-Crespo, A., Garnavich, P. M., Curiel, S. Raga, A. C., & Ayala, S. 1997, ApJ, 486, L55

Ogura, K. 1995, ApJ, 450, L23

Pravdo, S. H., Rodriguez, L. F., Curiel, S., Cantó, J., Torrelles, J. M., Becker, R. H., & Sellgren, K. 1985, ApJ, 293, L35

Raga, A. C., Barnes, P. J., & Mateo, M. 1990, AJ, 99, 1912

Reipurth, B., Heathcote, S., Roth, M., Noriega-Crespo, A., & Raga, A. C. 1993, ApJ, 408, L49

Rodríguez L.F., Ho, P.T.P, Torrelles, J.M., Curiel, S., & Cantó, J. 1990, ApJ, 349, 645

Torrelles, J. M., Gómez, J. F., Ho, P. T. P., Rodríguez, L. F., Anglada, G. & Cantó, J., 1994, ApJ, 435, 290.

This manuscript was prepared with the AAS LATEX macros v4.0.

Figure Captions

Fig. 1.— Antenna temperature (in K) as a function of velocity (in km s^{-1}), at selected positions along the optical jet of the HH 1-2 system. In each panel the upper plot corresponds to the ^{12}CO emission at 1 MHz resolution, shifted and enlarged by a factor 10 in intensity to show the high velocity wings. The middle line is the ^{12}CO emission at 100 KHz resolution, and the histogram is the ^{13}CO emission at 100 KHz.

Fig. 2.— **(a)** A series of ^{12}CO J=2-1 maps at different velocity channels of the HH 1-2 outflow, covering a region of 316″ × 440″. The optical knots are overlaid in black and labels for some of the sources and the HH object present in the region are included. The upper grey scale limits are different for each frame, in order of increasing velocity: 10, 20, 50, 75, 15, 10, 10, 20, and 20. The contours for the maps are: ¿from 1 to 3 by 1; 6 to 14 by 2; 25 to 35 by 2; 36 to 51 by 3; 3 to 8 by 1; 1.5 to 6.5 by 1; 1 to 5 by 1; 3 to 12 by 2; 1.5 to 6.0 by 1 (K km s^{-1}). **(b)** ^{13}CO emission at selected velocity ranges. The contours are the following: from 5 to 22.5 by 2.5; 7 to 27 by 2.5; 2 to 12 by 2 (K km s^{-1}). **(c)** A superposition of the ^{12}CO $J = 2 - 1$ and the optical [S II] 6717/31 emissions from Reipurth et al. (1993) within a 2′ field of the HH 1−2 system. The contours are logarithmic and for a velocity range of 11-11.5 km s^{-1}, the ambient gas is at a velocity of 9.5 km s^{-1}.

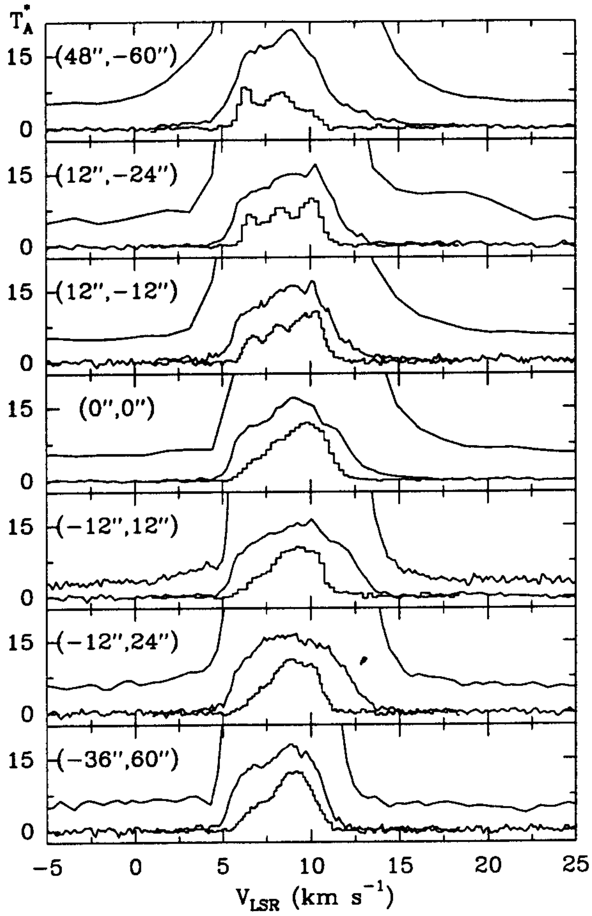
T_A^*
15
0
(48″,−60″)
(12″,−24″)
(12″,−12″)
(0″,0″)
(−12″,12″)
(−12″,24″)
(−36″,60″)
−5
0
5
10
15
20
25
V_{LSR} (km s^{-1})

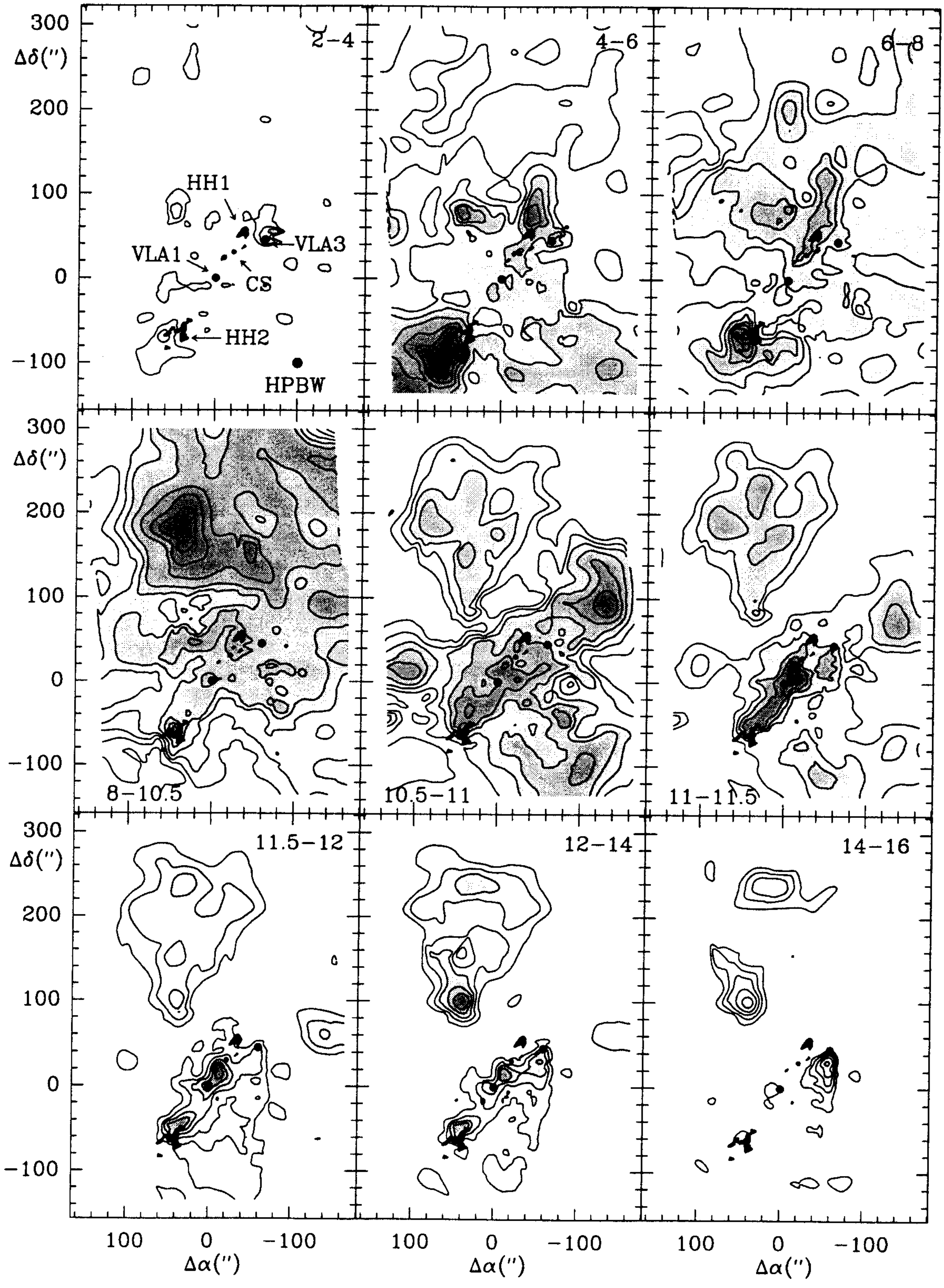
2–4
4–6
6–8
HH1
VLA1
VLA3
CS
HH2
HPBW
8–10.5
10.5–11
11–11.5
11.5–12
12–14
14–16
300
200
100
0
−100
Δδ('')
100
0
−100
Δα('')

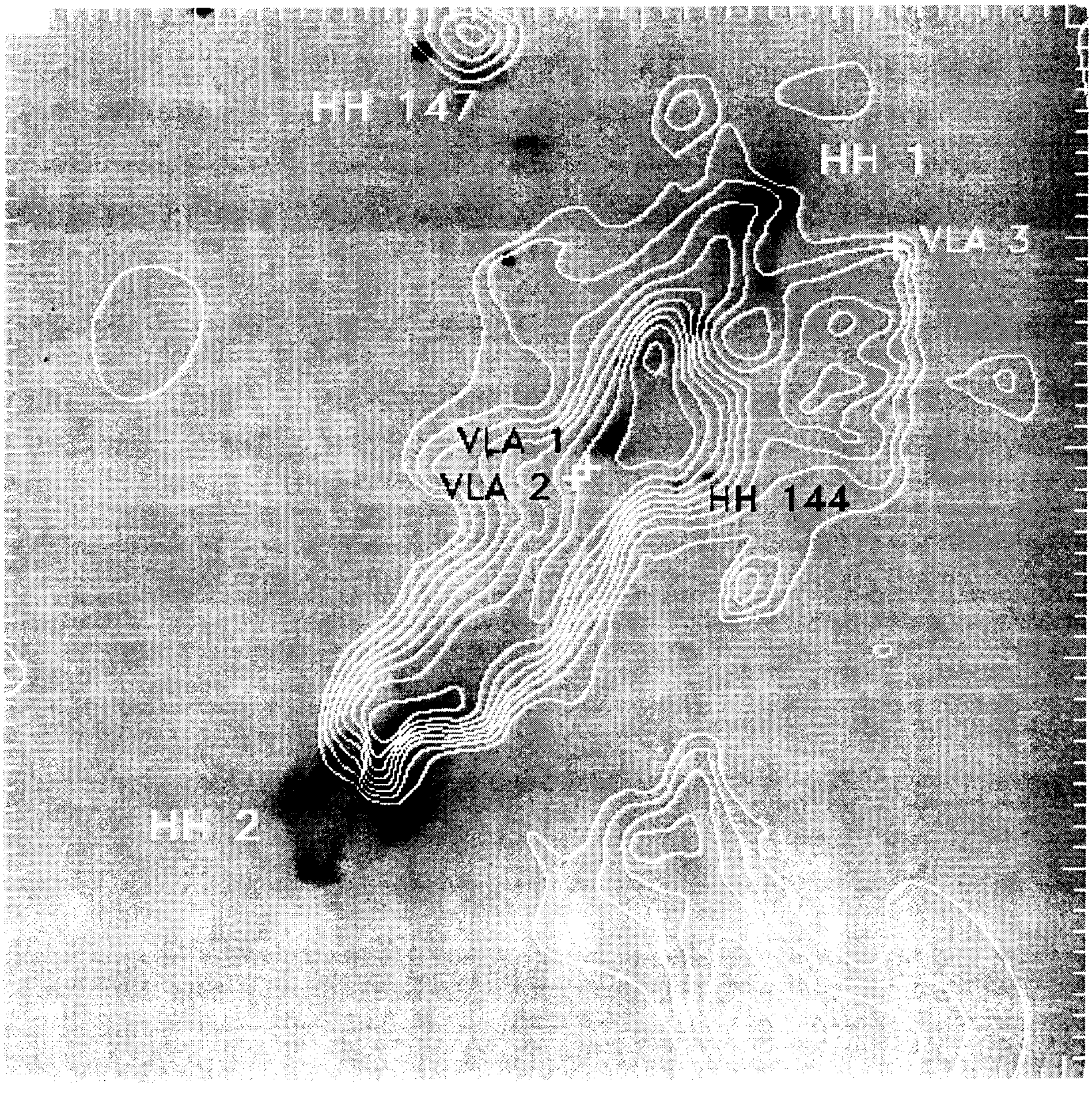

HH 147
HH 1
VLA 3
VLA 1
VLA 2
HH 144
HH 2

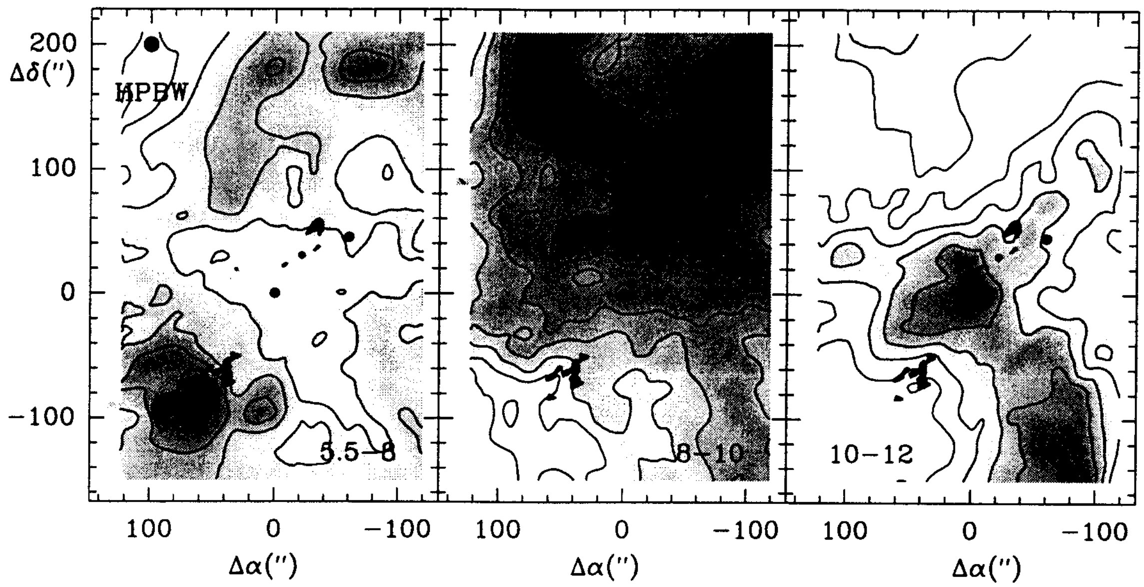
200
Δδ('')
HPBW
100
0
−100
5.5−8
8−10
10−12
100
0
−100
Δα('')